Polarization of ^{169}Tm and ^{19}F in CaF$_2$:Tm^{2+} by Optical Pumping*

William B. Grant,† L. F. Mollenauer, and C. D. Jeffries

Physics Department, University of California, Berkeley, California 94720

(Received 25 March 1971)

Nuclear polarization of ^{169}Tm $(I=\frac{1}{2})$ is achieved in a crystal of CaF$_2$ containing a small fraction of paramagnetic Tm^{2+} ions $(S=\frac{1}{2})$ by optically pumping with circularly polarized light in the region 5400–6000 Å, where there is a large magnetic circular dichroism. By optical pumping alone at $T=1.65\,°$K and in a field $H=750$ G a nuclear polarization of 9% is observed. If the $I_+ S_-$ rf transition is simultaneously saturated, the polarization increases to 18%. The polarization is reversed by changing from left- to right–circularly polarized light. These results are understood in terms of a model in which a large degree ($\sim$90%) of nuclear-spin memory exists in the optical-pumping cycle. The experiment proves the feasibility of significant nuclear polarizations in solids by optical pumping. A small polarization of the abundant ^{19}F nuclei is produced by a three–spin cross-relaxation process with two optically pumped ^{169}Tm^{2+} ions.

I. INTRODUCTION

Methods in use for orienting nuclei in solids, broadly classed into thermal-equilibrium methods and dynamic methods, generally require temperatures in the range 1–$10^{-2}\,°$K, usually high magnetic fields, and also microwave pumping for the dynamic methods. Oriented samples of nuclei are of considerable utility in solid-state, nuclear, and elementary-particle physics; we refer to some reviews[1,2] for details; the results have certainly justified the experimental complexity required.

On the other hand, in gases it is well known that the idea of optical pumping, introduced by Kastler,[3,4] is a relatively simple room-temperature method, and in certain substances, notably ^{3}He gas, a special technique has lead to sizable and useful nuclear polarizations.[5] The idea that nuclei in solids might be polarized by optical pumping had been considered,[6-8] but no successful experiments were reported, although the important work of Karlov, Margerie, and Merle-D'Aubigne[7] on F centers suggested that it might be possible. A re-examination of the mechanisms involved, and, in particular, resonance and relaxation in the ground state of paramagnetic species in solids, led us to propose several specific schemes,[9] with these general features: production of electron-spin polarization by pumping with, say, circularly polarized light; transfer of this polarization to nuclei through any of several phenomena: hyperfine (hfs) coupling, selective spin-lattice relaxation processes, saturation of microwave transitions, or multispin cross relaxation. The schemes are essentially mixtures of ideas from optical pumping in gases and microwave dynamic polarization in solids. The justification for considering such schemes is that nuclei not amenable to other methods may be oriented, and that in principle, if not yet in practice, sizable

polarizations are possible at room temperature, in contrast to existing methods for solids, where the polarization is determined by Boltzmann factors $e^{E/kT}$, which can only be made large enough at low temperatures.

The advent of the solid-state laser has greatly stimulated the development and study of crystals that can be optically pumped. In particular the detailed studies by Anderson, Weakliem, and Sabisky[10] of the magnetic circular dichroism (MCD) of CaF$_2$:^{169}Tm^{2+} led us to use this crystal to achieve the first significant nuclear polarization in a solid by optical pumping, briefly reported earlier.[11] In this paper we give fuller details and report a higher polarization $P_n(^{169}$Tm$)=18\%$, as well as a small polarization of the abundant ^{19}F nuclei. Small polarizations of order $10^{-3}\%$, have been obtained by optical pumping for ^{29}Si in silicon by Lampel[12] by a method similar to that discussed here, and for protons in anthracene by Maier *et al.*[13] through a rather different mechanism involving spin-selective deexitation to an excited triplet.

To fix ideas in a simple resumé of our method, consider a CaF$_2$ crystal containing about 0.05% ^{169}Tm^{2+} ions, which substitute for Ca^{2+} in the lattice. In a magnetic field H the effective-spin Hamiltonian of the electronic ground state is[14]

$$\mathcal{K}=g\mu_B \vec{H}\cdot\vec{S}+A\vec{I}\cdot\vec{S}-g'_n\mu_B\vec{H}\cdot\vec{I}.\qquad(1)$$

The first term is the Zeeman interaction of a spin $\vec{S}$, representing a Tm^{2+} ion with isotropic g factor; $S=\frac{1}{2}$ and μ_B is the Bohr magneton. The second term is the hfs interaction of $\vec{S}$ with a nuclear spin $\vec{I}$, representing ^{169}Tm, 100% naturally abundant, with $I=\frac{1}{2}$. The third term represents the nuclear Zeeman interaction, and will be neglected. In a large field the states are well described by the basis states $|M_S M_I\rangle$, where $M_S=\pm\frac{1}{2}$, $M_I=\pm\frac{1}{2}$; the notation is shortened to $|++\rangle$, etc., in Fig. 1,

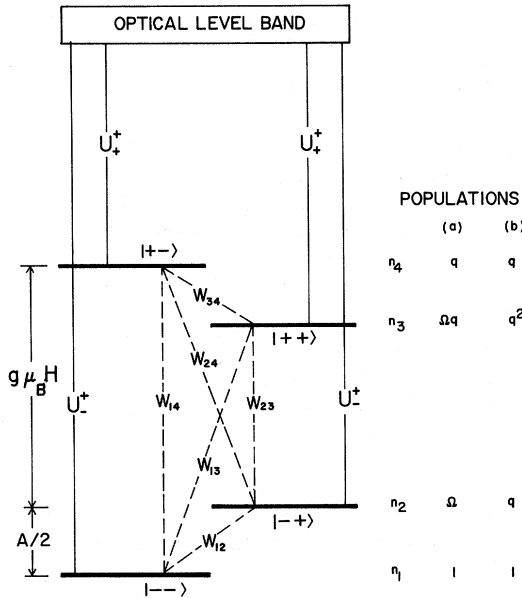FIG. 1. Energy levels for the ^{169}Tm^{2+} hyperfine system in a large magnetic field, showing optical pumping rates $U_{\pm}^+$ for σ^+ polarized light, spin-lattice relaxation rates w_{ij}, and populations achieved by optical pumping and rf.

which shows the energy levels, relative populations n_i, as well as spin-lattice relaxation rates w_{ij} between the various levels, and an optical level or band to which we induce transitions by illuminating the crystal with circularly polarized light. Assume that pumping with right-hand (σ^+) light induces transitions at the rates U_+^+ and U_-^+, as shown, where the superscript refers to σ^+ light and the subscript to the sign of M_S. The important point is that U_+^+ and U_-^+ may be significantly different. This comes about because the light wave is coupled only to the electrons and the transitions obey the selection rule $\Delta M_I = 0$, $\Delta M_J = +1$, where J is the true angular momentum, not the effective spin. The exact values of U_+^+ and U_-^+ depend on the detailed make-up of the true ground state and excited-state wave functions, but it suffices at this point to simply state that CaF$_2$:Tm^{2+} has an unusually large MCD and that $(U_-^+/U_+^+) \approx 0.6$ at visible wavelengths. [10] It is not unreasonable to assume a reasonably large degree of nuclear-spin memory (i.e., $\Delta M_I = 0$) in the complete pumping cycle because the nuclei are only weakly coupled to the lattice. This means that ions pumped up from the left-hand side of Fig. 1 will return to the left-hand side, etc. We also postulate that the electron spins are likely to become thermalized and the optical decay is equally likely to either $M_S = +\frac{1}{2}$ or $-\frac{1}{2}$ states, i.e., no electron-spin memory exists. The net effect of strong optical pumping is to establish the populations of Fig. 1, column (a), where, by detailed balance,

$(n_4/n_1) \rightarrow (U_-^+/U_+^+) \equiv q$, $(n_3/n_2) \rightarrow q$, and Ω is to be determined by transitions between the left- and right-hand sides of Fig. 1. Suppose that the "forbidden" transition W_{24} is strongly saturated by an rf oscillator; this is, in fact, commonly done in microwave dynamic polarization. [15] This equalizes populations n_4 and n_2, i.e., $\Omega \rightarrow q$, yielding the populations of column (b), Fig. 1, and an enhanced nuclear polarization

$$P_n = \frac{\langle I_z \rangle_{av}}{I} = \frac{n_3 + n_2 - n_1 - n_4}{n_3 + n_2 + n_1 + n_4} = \frac{q-1}{q+1} = \frac{U_-^+ - U_+^+}{U_-^+ + U_+^+} , \tag{2}$$

which is just equal to the enhanced electron polarization

$$P_e = \frac{\langle S_z \rangle_{av}}{S} = \frac{n_4 + n_3 - n_2 - n_1}{n_4 + n_3 + n_2 + n_1} = \frac{q-1}{q+1} = \frac{U_-^+ - U_+^+}{U_-^+ + U_+^+} . \tag{3}$$

For $q = (U_-^+/U_+^+) \approx 0.6$, as for CaF$_2$:Tm^{2+}, this predicts $P_n \approx P_e \approx -25\%$. Since by definition the thermal-equilibrium values of P_n and P_e are negative, this is a "positive enhancement." Furthermore q is determined by matrix element ratios for optical transitions and is independent of the temperature; this means that Eq. (2) applies even at room temperature, provided that optical and rf saturation can be maintained. If left-hand circularly polarized light (σ^-) is used instead of σ^+ light, $q \rightarrow q^{-1}$ because of the Kramers theorem, and P_n and P_e are reversed in sign from Eqs. (2) and (3). Using σ^+ light, P_n may be reversed by saturating W_{13} instead of W_{24}, but P_e is not reversed.

Another variation is to utilize the fact that it is possible to have quite unequal relaxation rates, say $w_{24} \gg w_{13} \gg w_{12} = w_{34}$, as is known from microwave dynamic polarization studies. [15] Then, without rf saturation, this makes $\Omega = q\, e^{g\mu_B H/kT} = q e^{\Delta}$, and

$$P_n = \frac{q - e^{-\Delta}}{q + e^{-\Delta}} . \tag{4}$$

If, on the other hand, we assume $w_{13} \gg w_{24}$, P_n is reversed. At room temperature Eq. (4) becomes Eq. (2). We have been assuming $g\mu_B H \gg A$ up until now, but, as shown in Sec. IV, similar conclusions hold in low fields where the hfs term is dominant; it is also shown that nuclear-spin memory is not essential.

It is worth noting that at very low temperatures where $q \gg e^{-\Delta}$, $P_n \rightarrow 100\%$, even if $q = 1$, i.e., for unpolarized light. This is not a new result, it is just an optically pumped version of Abragam's [16] generalization of the Overhauser effect [17]; it tends to saturate P_e to zero and probably would have no advantage over the microwave method. As such, it is basically different from the schemes con-
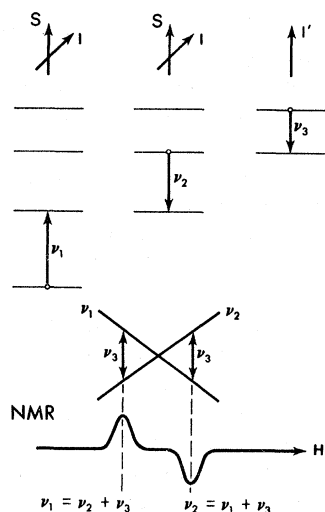
FIG. 2. Scheme for polarizing abundant nuclei I' by three-spin cross relaxation with two Tm^{2+} ions.

sidered above, where the angular momentum from the circularly polarized photon itself is eventually transferred to the nuclear spin.

Since we are concerned principally with the schemes leading to Eqs. (2) and (4) it is well to point out that the principal experimental difficulty in solids is to find samples which satisfy two conditions: (i) The rates U_+^* and U_-^* are sufficiently different, i.e., a large MCD; and (ii) where U_+^*, $U_-^* \gg w_{ij}$ and $W_{rf} \gg w_{ij}$, in order that optical and rf saturation can be achieved. These conditions are somewhat incompatible since condition (i) requires a large spin-orbit coupling for the character of the bands to be well resolved; but a large spin-orbit coupling generally increases w_{ij}, making it difficult to achieve condition (ii). Although there may well be samples for which these two conditions can be achieved at room temperature (e.g., F centers), in the reported experiments on $CaF_2:Tm^{2+}$ we have resorted to working at helium temperatures in order to reduce w_{ij} comparable to rates $U_\pm$ and W_{rf} obtainable with pumping with a simple mercury arc lamp, and a low-power rf signal generator, respectively.

It was also proposed[9] that multispin relaxation could be used to transfer the optically pumped polarization of the $\vec{S}$, $\vec{I}$ hyperfine system (e.g., $^{169}Tm^{2+}$) to the abundant nuclei $\vec{I}'$ in the crystal at diamagnetic sites (e.g., ^{19}F), as indicated schematically in Fig. 2, which shows two neighboring $^{169}Tm^{2+}$ ions and an ^{19}F nucleus. At a certain field where $\nu_1 = \nu_2 + \nu_3$, just below the crossing of the ν_1 and ν_2 hfs frequencies, we may have energy-conserving spin flips in which one ion flips up, the second down, and ^{19}F flips down, thus enhancing the ^{19}F nuclear polarization. At a slightly

higher field where $\nu_2 = \nu_1 + \nu_3$, the ^{19}F polarization will be reversed and enhanced. We have observed such three-spin cross-relaxation behavior,[18] and will give a fuller discussion in Sec. VI.

The contents of this paper are discussed more fully in Grant's thesis.[19]

II. PROPERTIES OF CaF_2:$^{169}Tm^{2+}$

Single crystals of $CaF_2:Tm^{3+}$ are grown by the Bridgman-Stockbarger[20] technique. The Tm^{3+} may be reduced to Tm^{2+} by x irradiation,[21] γ irradiation,[22] electrolytic reduction,[23] or calcium baking,[24] the latter being preferable. The Tm^{2+} occupies a Ca^{2+} site of O_h cubic symmetry. Unreduced Tm^{3+} may have cubic or axial symmetry, depending on whether the charge compensation is remote or local[25]; the cubic site presumably has a singlet lowest level and is nonmagnetic. Paramagnetic resonance experiments on the two crystals we used, Table I, revealed only the Tm^{2+} resonance.
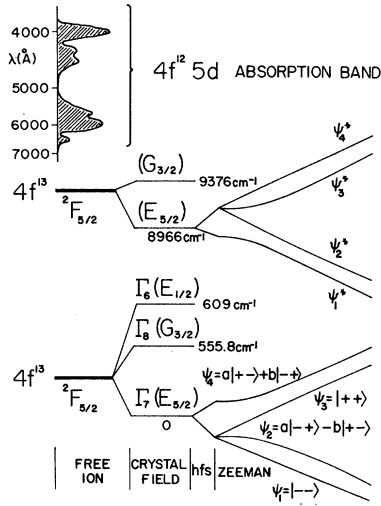
A. Energy Levels

$CaF_2:Tm^{2+}$ has been well studied: optical absorption,[26] paramagnetic resonance in the ground state[14,21] and metastable state,[27] crystal-field theory,[28] MCD,[10] optical pumping,[29] and spin-lattice relaxation.[30,31] The pertinent energy levels are shown in Fig. 3.

Tm^{2+} has a $4f^{13}$ configuration, with a $^2F_{7/2}$ ground-state multiplet and a $^2F_{5/2}$ excited-state multiplet, which is higher by 9000 cm^{-1} because of the unusually large spin-orbit coupling. The O_h crystal field of CaF_2 splits the degenerate ground state of the free ion into a lowest Kramers doublet Γ_7, a Γ_8 quartet at 555.8 cm^{-1}, and a doublet Γ_6 at 609 cm^{-1}.[31] These are also labeled $E_{5/2}$, $G_{3/2}$, and $E_{1/2}$, respectively, in the group notation of McClure, Polo, and Weakleim.[32] Figure 3 shows the $E_{5/2}$ ground doublet further split by hfs and by a magnetic field, giving the four levels previously shown in Fig. 1. The ground-state spin Hamiltonian parameters in Eq. (1) are measured to be[14] $g = +3.453 \pm 0.003$, $A/h = -(1101.376 \pm 0.004)$ MHz, and $g_n' = 0.41 \times 10^{-3}$.

TABLE I. CaF_2: Tm^{2+} crystals used.

	Sample No. 1	Sample No. 2
%Tm	0.05%	0.05%
Source	Edelstein	Edelstein
Reduction method	Calcium baking	Electrolytic
Orientation of H	[111]	[111]
% reduced	50%	40%
Other centers	M centers, Ho^{2+}	Ho^{2+}

FIG. 3. Energy levels of CaF$_2$: ^{169}Tm^{2+}.

The transition frequencies ν_{ij} between pairs of levels are shown in Fig. 4.

The upper $^2F_{5/2}$ multiplet is split by the crystal field into a $\Gamma_8(G_{3/2})$ quartet and a $\Gamma_7(E_{5/2})$ doublet at 8966 cm^{-1}, which is metastable with a lifetime of 5 msec and gives useful laser emission lines. Roughly 1% of the optical decay is via this metastable state, and under our pumping conditions virtually all population resides in the ground state. The spin Hamiltonian parameters for the metastable level are[27] $g = -1.453$ and $A/h = +1160$ MHz; the transition frequencies ν_{ij}^* are shown in Fig. 4.

Also shown in Fig. 3 is the visible part of $4f^{12}5d$ band, to which we pump. The important quantity for our purposes is U_-^*/U_+^*, which is related to the MCD measured by Anderson et al.,[10] in terms of the low-temperature saturated ellipticity[33]

$$\Theta_\infty(\lambda) \equiv (\alpha^+ - \alpha^-)/(\alpha^+ + \alpha^-) \ , \tag{6a}$$

where $\alpha^\pm$ is the optical-absorption coefficient for $\sigma^\pm$ circularly polarized light at wavelength λ, extrapolated to $(H/T) \to \infty$, where only the $|--\rangle$ state, Fig. 3, is populated. The latest result[33] for orientation $\vec{H}\parallel[111]$ shows there is a negative peak $\Theta_\infty \approx -0.3$ at 4120 Å, and another broader peak $\Theta_\infty \approx -0.32$ at 5400–5800 Å; these peaks are used in our experiments for monitoring and pumping, respectively. Since only $M_S = -\frac{1}{2}$ states are populated as $(H/T) \to \infty$, absorption occurs only from these states, and in Eq. (6a) we replace $\alpha^\pm$ by $\alpha_-^\pm$, the subscript denoting the sign of M_S. From the Kramers theorem, $\alpha_+^+ = \alpha_-^-$ and $\alpha_-^+ = \alpha_+^-$. The transition rate is just proportional to the absorp-

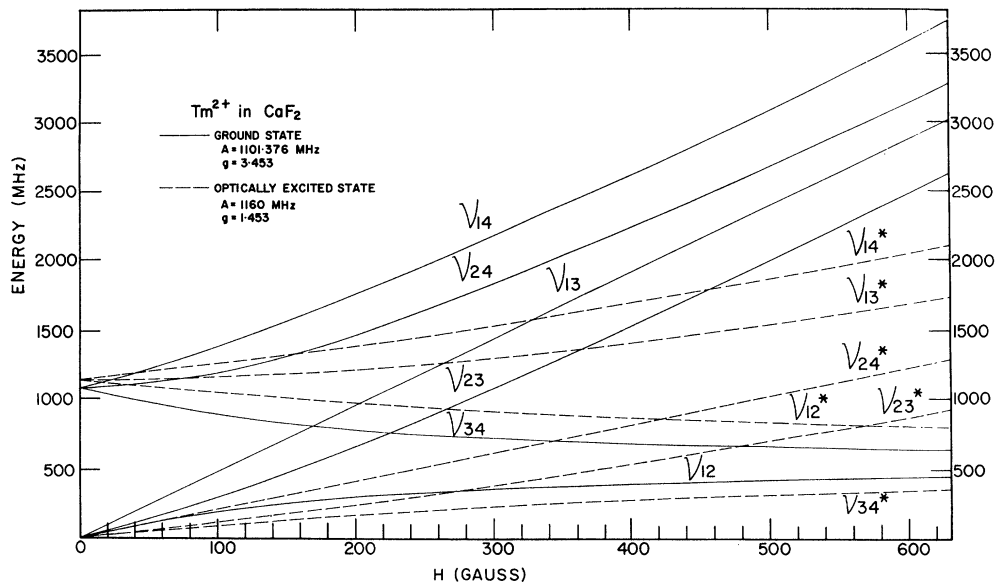Using these values and neglecting the g_n' term we have diagonalized Eq. (1) to obtain the energy levels shown, and the effective-spin eigenfunctions $|M_S M_I\rangle$

$$\psi_1 = |--\rangle, \tag{5a}$$

$$\psi_2 = a|-+\rangle - b|+-\rangle, \tag{5b}$$

$$\psi_3 = |++\rangle \ , \tag{5c}$$

$$\psi_4 = a|+-\rangle + b|-+\rangle \ , \tag{5d}$$

where $a^2 + b^2 = 1$ and

$$a = A\left\{2A^2 + 2(g\mu_B H)^2 - 2g\mu_B H[A^2 + (g\mu_B H)^2]^{1/2}\right\}^{-1/2} \ . \tag{5e}$$

FIG. 4. Frequencies ν_{ij} between the hfs levels of CaF$_2$: ^{169}Tm^{2+} for the ground state $^2F_{7/2}(E_{5/2})$; and ν_{ij}^* for the metastable state $^2F_{5/2}(E_{5/2})$ at 8966 cm^{-1}.
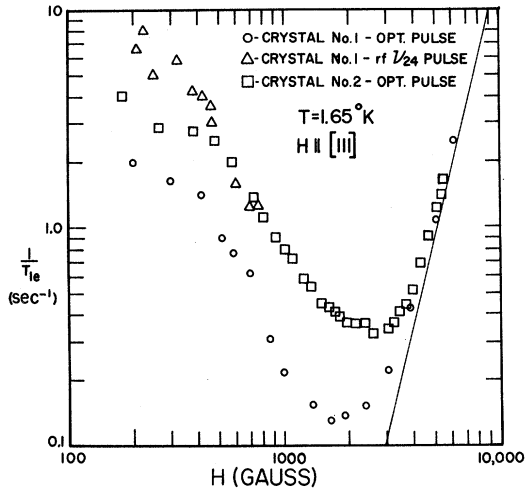
FIG. 5. Measured relaxation rate T_{1e}^{-1} for recovery of MCD signal following an optical or rf pulse for CaF_2:$^{169}Tm^{2+}$ crystals, Table II. The solid line is the first term of Eq. (9).

tion coefficient, i.e., $U_{\pm}^{\pm} \propto \alpha_{\pm}^{\pm}$, and hence

$$\Theta_{\infty} = \frac{\alpha_-^+ - \alpha_-^-}{\alpha_-^+ + \alpha_-^-} = \frac{\alpha_-^+ - \alpha_+^+}{\alpha_-^+ + \alpha_+^+} = \frac{U_-^+ - U_+^+}{U_-^+ + U_-^+} = \frac{q-1}{q+1} \ ,$$

(6b)

showing that the maximum value of the nuclear and electron polarization, Eqs. (2) and (3), is just given by the ellipticity Θ_{∞}.

The oscillator strength is of order 10^{-2}–10^{-3} for these Tm^{2+} $4f$-$5d$ transitions. This is much larger than the oscillator strengths of the $4f$-$4f$ transitions, which are the only transitions in the visible region for trivalent rare-earth ions.

B. Spin-Lattice Relaxation

For the Kramers doublet such as the $E_{5/2}$ ground state of magnetically dilute Tm^{2+}, the dominant spin-lattice relaxation is due to the thermal modulation of the crystalline electric field, leading to a relaxation rate of the form[34,35]

$$T_{1e}^{-1} = A H^4 T + C T^9 \ , \tag{7}$$

for the direct and Raman processes, respectively. Huang's[30] measurements on CaF_2:0.2% Tm^{2+} at 8.9 kMHz using the microwave paramagnetic resonance pulse-recovery method yielded for $H \approx 2$kG, $\vec{H} \parallel [100]$

$$T_{1e}^{-1} = 13T + 7.7 \times 10^{-8} T^9 \ \text{sec}^{-1} \ . \tag{8}$$

Sabisky and Anderson[31] later made measurements of T_{1e} by monitoring the recovery of the MCD signal following a disturbance by a pulse of microwaves, or light, or heat. They used Tm concentrations in the range 0.01–0.0067% and varied H

from 1 to 10 kG. For $H > 2$kG they found for $\vec{H} \parallel$ [100]

$$T_{1e}^{-1} = (5.6 \pm 0.05) \times 10^{-4} H^4 T$$

$$+ (7.6 \pm 0.7) \times 10^{-8} T^9 \ \text{sec}^{-1}, \tag{9}$$

where T is in $^{\circ}$K and H is in kG. They also found that the direct process depended slightly on crystal orientation. While Eqs. (8) and (9) are in agreement for the Raman rate, the first term in Eq. (8) is three orders of magnitude larger than that in Eq. (9), which we feel represents the true direct process. Huang's first term represents cross relaxation. In fact, Sabisky and Anderson also found a bad scatter in the data below 2 kG, concentration dependent, and no doubt due to cross relaxation. The measured rates in Eq. (9) are in moderate agreement with theoretical estimates.[31]

We have measured T_{1e}^{-1} for the two crystals of Table I with the results shown in Fig. 5. The methods used were to monitor the recovery of the MCD signal following a saturating pulse of light or an rf pulse at ν_{24}. The latter measurements were done $2\frac{1}{2}$ years earlier and appear to give a faster relaxation rate by a factor 2 than the optical-pulse method, possibly because the rf pulse only saturates a packet in the inhomogeneously broadened line, followed by spectral diffusion, which is difficult to distinguish from spin-lattice relaxation and usually yields faster over-all recovery times. At fields above 3 kG our data agree with the first term of Eq. (9), and at low fields of ≈ 500 G, where the polarization experiments were performed, the observed rate is about four orders larger than the true direct rate. In fact, at 1.65 $^{\circ}$K both the Raman relaxation time and the true direct relaxation time are $\sim 10^5$ sec, which is so long that it is not at all surprising that they are completely masked by cross relaxation.

The rate T_{1e}^{-1} of Fig. 5 represents roughly the average of the rates w_{14} and w_{23} introduced in Fig. 1. We have no direct experimental measurements of the rates w_{13}, w_{24}, w_{12}, and w_{34}. We calculate theoretically the rates w_{ij} for the direct process in the Appendix, with the results shown in Fig. 6, assuming $T = 1$ $^{\circ}$K. The calculation is an extension of that of Sabisky and Anderson,[31] taking into account the hfs, and agrees at high field with their result, i.e., $w_{14} = w_{23} = T_{1e}^{-1}$. Unfortunately at our fields of interest, ~ 500 G, the rates w_{ij} in Fig. 6 are completely swamped by cross relaxation, so that this calculation cannot be used in Sec. IV to predict the nuclear polarization by optical pumping.

III. APPARATUS AND PROCEDURES

Although Eqs. (2) and (3) adequately define the nuclear and electron polarization at high fields
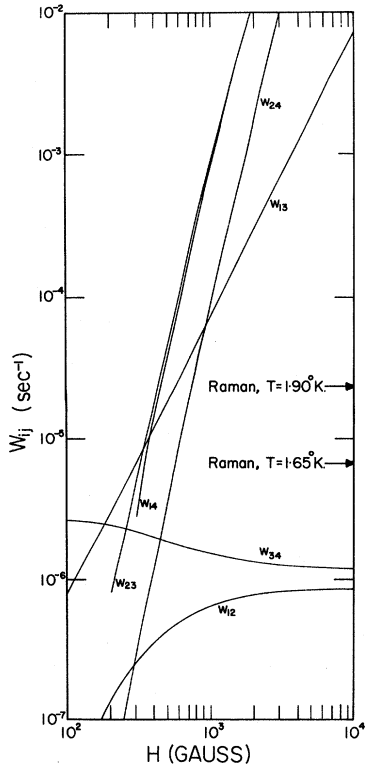
FIG. 6. Relaxation rates w_{ij} at 1 °K for CaF$_2$: ^{169}Tm^{2+} as calculated in the Appendix. Raman rates, for reference, are calculated from Eq. (9).

(Fig. 1) we actually work in intermediate fields (Fig. 3) where the wave functions are given by Eqs. (5) in terms of the coefficients a and b. Taking the sum of the ground-state populations $n_1 + n_2 + n_3 + n_4 = 1$ for normalization we can write, in general,

$$P_n = n_3 - n_1 - (a^2 - b^2)(n_4 - n_2) \ , \tag{10a}$$

$$P_e = n_3 - n_1 + (a^2 - b^2)(n_4 - n_2) \ . \tag{10b}$$

The apparatus required must pump the crystal optically and with rf fields, and provide a means for measuring P_e and P_n. Figure 7 shows the arrangement chosen: P_e and P_n are enhanced by pumping the crystal with circularly polarized light (σ^+ or σ^-) in the range 5400–6000 Å from a mercury arc lamp; a weak monitor beam at 4120 Å, switched rapidly between σ^+ and σ^-, is used to measure P_e and P_n, as described below.

The CaF$_2$:Tm^{2+} crystal, 5×3×1.5 mm thick, was mounted on a holder and inserted into a stainless-steel liquid-He^4 Dewar with strain-free fused-quartz windows.[36] Fields of up to 1 kG were provided by copper-foil Helmholtz coils outside the Dewar. Fields up to 55 kG were provided by a small super-conducting solenoid with a 9-mm bore, mounted directly on the sample holder and cooled by the sample helium bath, usually down to $T \approx 1.65$ °K.

The optical pumping arrangement was a 200-W high-pressure Hg arc (PEK Labs type 203); a 75-mm-diam special f/1.0 aspheric quartz lens; a dichroic mirror (Liberty Mirror type 90-580) which reflected light in the 5000–6000-Å region; Corning glass filters (types 3-69 and 3-70) to block light of $\lambda < 4900$ Å; a Polaroid (type HNCP37) laminated plastic circular polarizer; and a 125-mm-focal-length lens to focus the lamp image onto the crystal, where the light intensity was about 2 W/cm^2.

The monitor-beam light came from a 75-W xenon arc lamp (PEK Labs type x-76); a monochrometer (Jarrell-Ash One Meter Czerny-Turner Spectrometer); a collimating lens; a Glan-Thompson linear polarizer; a quartz quarter-wave plate, oscillating sinusoidally through $\pm \frac{1}{4}\lambda$ at 17 kHz, described earlier[37]; focusing lens onto crystal; 90° prism; interference filter to pass 4120 Å; and photomultiplier (EMI type 9558 Q/B). In later experiments we used an oscillating $\pm \frac{1}{4}\lambda$ plate developed by Kemp[38] at 50 kHz, and also stabilized the average photomultiplier output voltage V_{dc} at point Q by a feedback loop, in order to eliminate noise from low-frequency light intensity fluctuations and to facilitate measurement of S, Eq. (11). The ac signal voltage V_{ac} from the photomultiplier was amplified by a lock-in detector and displayed either on a chart recorder, an oscilloscope, or a 1024 channel signal averager (Nuclear Data Co. Enhancetron). On the whole, the optical pumping and monitoring technique is related to that used by Parry *et al*.[38a]

A loop of wire around the crystal was connected to various cw and pulsed-signal generators in the range 0.2–4 GHz for inducing rf transitions, in particular ν_{24}, Fig. 3.

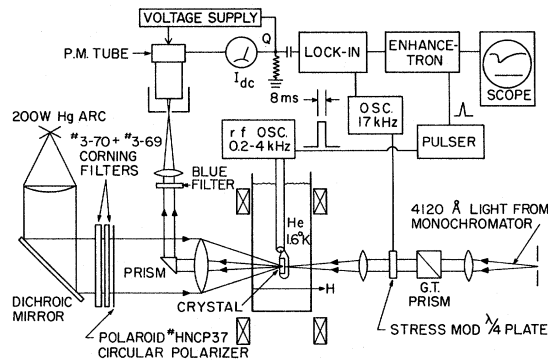The signal that we measure with the monitor beam, often called the "MCD signal," is defined by

FIG. 7. Apparatus used for optical pumping and monitoring the MCD signal.

$$S = \frac{I^+ - I^-}{I^+ + I^-} = \frac{V_{ac}}{V_{dc}} , \qquad (11)$$

where I^+ and I^- are the peak photomulitplier currents that occur periodically as the beam oscillates between pure σ^+ light and pure σ^- light. It can be shown[11,19,31] for weak differential absorption, where $\exp[P_e(\alpha_+^* - \alpha_-^*)\ell] \approx 1 + P_e(\alpha_+^*)\ell$, for cyrstal thickness ℓ, that S can be written as

$$S = \tfrac{1}{2}(\alpha_-^* + \alpha_+^*)\ell \, \Theta_\infty P_e = KP_e . \qquad (12)$$

The first factor is just the total-absorption coefficient for unpolarized light for the crystal in zero field, and depends only on the wavelength and the Tm^{2+} concentrations; Θ_∞ depends only on λ. Thus the signal S for a given crystal at constant λ is directly proportional to P_e, the electron-spin polarization, Eq. (10b); the calibration factor K can be directly measured by taking for P_e the thermal-equilibrium value $P_{eB} = -\tanh(g\mu_B H/2kT)$ $\approx -\tanh(g\mu_B H/2kT)$ in a known field and temperature. Equation (12) is valid for any spin temperature, and furthermore, it holds for any value of the wave-function admixture coefficients a and b.

Actually, $KP_e \propto H/T$ in Eq. (12) represents only the paramagnetic circular dichroism, and there should be added a diamagnetic term CH, proportional to the field but independent of temperature. This term is significant in, say, F centers,[39] but for $CaF_2 : Tm^{2+}$ it is only of order 10^{-4} at 1 kG and can be neglected.[19]

Since the direct NMR signal of the dilute ^{169}Tm nuclei is far too weak to be observable, we used the following optical method for measuring P_n. First, we measure the MCD signal $S = S_B$ at thermal equilibrium in H and T; then the optical pump is turned on and the "pumped" signal S_p is measured, yielding a pumped electron polarization

$$P_{ep} = -(g\mu_B H/2kT)(S_p/S_B). \qquad (13)$$

We then apply a short saturating pulse at ν_{24}, which gives an instantaneous signal S_{pi24}. From Fig. 1 the pulse makes $n_2 = n_4$ and leaves n_1 and n_3 undisturbed, provided the pulse length τ is short compared to optical-pump time $(U^*)^{-1}$ and relaxation time w_{ij}^{-1}; $\tau \approx 10^{-2}$ sec was short enough in all cases. Then, from Eqs. (10), P_n just prior to the pulse is given by

$$P_{ni} = -(g\mu_B H/2kT)(2S_{pi24} - S_p)/S_B . \qquad (14)$$

As a check on the use of Eq. (14), pulsed measurements were performed without prior optical pumping, and always yielded $2S_{pi24} = S_B$ and $P_{ni} = 0$, as expected since at thermal equilibrium $P_n \approx 10^{-4}$. We estimate that values of P_n measured by the procedure of Eq. (14) are correct to within 10%.

For schemes requiring continuous saturation of ν_{24}, we measured P_n by first measuring S_B; then
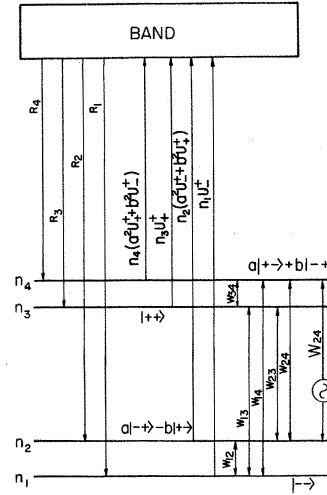

FIG. 8. Energy levels for $I = \tfrac{1}{2}$, $S = \tfrac{1}{2}$ hfs system, populations, wave functions in arbitrary field, optical pump rates up to band, and optical return rates R_i.

ν_{24} was turned on and the steady-state signal S_{p24} recorded. From Eqs. (10) with $n_2 = n_4$, one finds

$$P_{n\nu24} = -(g\mu_B H/2kT)(S_{p24}/S_B). \qquad (15)$$

The steady-state signals S_p, S_B, and S_{p24} were read from the lock-in output on a chart recorder. The instantaneous signal S_{pi24} was stored in the Enhancetron, and the pulse repeated at intervals of 5 sec; usually after about 200 cycles, a signal-to-noise ratio of $\sim 20 : 1$ was achieved. To verify full rf saturation of ν_{24}, runs were taken with the power an order of magnitude larger than that which produced no further change in S_{pi24} or S_{p24}.

IV. THEORY

In this section we set up rate equations and calculate the dynamic populations and the polarizations P_n and P_e for any general $I = \tfrac{1}{2}$, $S = \tfrac{1}{2}$ hfs system (but with particular reference to $CaF_2 : {}^{169}Tm^{2+}$) in terms of the various optical and rf pumping and relaxation rates affecting the fractional populations n_1, n_2, n_3, and n_4 of the ground-state hfs levels, shown again in Fig. 8; we assume effective-spin wave functions, Eqs. (5), valid for all fields. We assume circular polarized optical pumping rates U_+ and U_- sec^{-1} from $M_S = \pm \tfrac{1}{2}$ states, respectively. The ground-state relaxation rate w_{ij} sec^{-1} is theoretically given by Fig. 6; but since the measured values of T_{1e}^{-1} $\approx w_{14}$ are completely dominated by cross relaxation, unfortunately we do not really know the relative values of the w_{ij} and will try to make reasonable estimates. We assume rf pumping only at ν_{24}, at a rate w_{24} sec^{-1}; this is sufficiently representative of the effects to be expected by rf pumping.

Since the optical pump rate is small compared

to the decay rate out of the metastable level, the population in this level is small. We make the approximation that the actual population always resides in the four ground hfs levels, i.e., assume a constant value $n_1+n_2+n_3+n_4=1$. We introduce the optical decay rates R_i sec^{-1} as unknown parameters subject only to the condition that the total rate out of the band equals the total rate into the band. The decay is primarily by phonon rather than photon emission.[26,32] Neglecting cross relaxation for the present, the rate equations are, from Fig. 8,

$$\frac{dn_1}{dt} = -n_1 u_- + R_1 + w_{12}(n_2 - n_1 e^{-h\nu_{12}/kT})$$

$$+ w_{13}(n_3 - n_1 e^{-h\nu_{13}/kT}) + w_{14}(n_4 - n_1 e^{-h\nu_{14}/kT}), (16)$$

with very similar equations for $\dot{n}_2$, $\dot{n}_3$, and $\dot{n}_4$.

The solution of these equations for the populations $n_1, \ldots$ depends to an important degree on the relative optical return rates R_i. This question has been considered previously. Franzen[40] considered the cases of either complete reorientation or no reorientation of the total angular momentum $\vec{F}$ for gaseous sodium atoms. Imbusch et al.[41] demon-

strated the existence of electron-spin memory (i.e., $\Delta M_S = 0$) in the optical pumping cycle in ruby. Mollenauer et al.[42] discovered ~ 95% electron-spin memory in the optical pumping cycle of F centers in alkali halides and used this in a new method to measure for the first time the g factors of the relaxed excited states in KCl, KI, and KBr. Anderson and Sabisky[43] demonstrated the existence of large nuclear-spin memory (i.e., $\Delta M_I = 0$) for optical pumping in CaF$_2$:^{169}Tm^{2+} to the metastable level. In order to treat this question most generally we write the R_i in terms of four parameters, α, β, γ, and δ, normalized so that $\alpha+\beta+\gamma+\delta=1$. Our parameters differ in meaning somewhat from those used by others.[42,43] Taking $\alpha=1$ and $\beta=\gamma=\delta=0$ is defined to mean that $\Delta M_I=0$ throughout the pumping cycle and that the electrons have been so thermalized in the band that the ground states $M_S=+\frac{1}{2}$ and $M_S=-\frac{1}{2}$ are repopulated at equal rates; in short, complete nuclear-spin memory but no electron-spin memory exists. This case together with the three other extreme cases are summarized in Table II, and are defined exactly by these equations for R_i:

$$R_1 = \tfrac{1}{4}n_1 U_-(2\alpha + 2\beta + \gamma + 4\delta) + \tfrac{1}{4}n_2[2\alpha b^2 U_+ + 2\beta a^2 U_- + \gamma(a^2 U_- + b^2 U_+)] + \tfrac{1}{4}n_3\gamma U_+$$

$$+ \tfrac{1}{4}n_4[2\alpha a^2 U_+ + 2\beta b^2 U_- + \gamma\ (a^2 U_+ + b^2 U_-)], \quad (17a)$$

$$R_2 = \tfrac{1}{4}n_1 U_-(2\alpha b^2 + 2\beta a^2 + \gamma) + \tfrac{1}{4}n_2[(a^4 U_- + b^4 U_+)(2\alpha + 2\beta + 4\delta) + \gamma(a^2 U_- + b^2 U_+)] + \tfrac{1}{4}n_3 U_+(2\alpha a^2 + 2\beta b^2 + \gamma)$$

$$+ \tfrac{1}{4}n_4[(2a^2 b^2)(U_+ + U_-)(\alpha + \beta + 2\delta) + \gamma(a^2 U_+ + b^2 U_-)], \quad (17b)$$

$$R_3 = \tfrac{1}{4}n_1\gamma U_- + \tfrac{1}{4}n_2[2\alpha a^2 U_- + 2\beta b^2 U_+ + \gamma(a^2 U_- + b^2 U_+)] + \tfrac{1}{4}n_3 U_+(2\alpha + 2\beta + \gamma + 4\delta)$$

$$+ \tfrac{1}{4}n_4[2\alpha b^2 U_- + 2\beta a^2 U_+ + \gamma(a^2 U_+ + b^2 U_-)], \quad (17c)$$

$$R_4 = \tfrac{1}{4}n_1 U_-(2\alpha a^2 + 2\beta b^2 + \gamma) + \tfrac{1}{4}n_2[(2a^2 b^2)(U_+ + U_-)(\alpha + \beta + 2\delta) + \gamma(a^2 U_- + b^2 U_+)] + \tfrac{1}{4}n_3 U_+(2\alpha b^2 + 2\beta a^2 + \gamma)$$

$$+ \tfrac{1}{4}n_4[2(a^4 U_+ + b^4 U_-)(\alpha + \beta + 2\delta) + \gamma(a^2 U_+ + b^2 U_-)]. \quad (17d)$$

Lacking detailed knowledge of band wave functions, relaxation mechanisms, etc., it is not possible, a priori, to calculate the actual values of α, β, γ, and δ for the CaF$_2$:^{169}Tm^{2+} system. Instead, we consider each case in Table II separately, and use the values of R_i in Eqs. (17) to solve the rate equations, Eqs. (16), to predict P_n and P_e; then we compare predictions with the data in Sec. V.

A. Case $\alpha = 1$

To see the behavior in the limit of extremely strong optical pumping alone, we take in Eqs. (16) $W_{24}=0$, $w_{ij}=0$, R_i from Eqs. (17) with $\alpha=1$, $\beta=\gamma=\delta=0$. The resulting equations have a simple solution, yielding polarizations just given by Eqs. (2).

and (3). This result is valid for all values of the field except at $H \to \infty$, where the polarizations are not determined by optical pumping alone. It is interesting to note that complete nuclear-spin memory gives the maximum value of nuclear polarization at essentially all fields, even without rf saturation and independent of the w_{ij}, provided the optical pumping rate can be made large enough. If one next adds to the model the relaxation w_{24}, one finds P_n given by Eq. (4) for all fields. To more fully explore this model it is necessary to assume specific values of T, U_+, U_-, and w_{ij}. We take $(U_-/U_+) \equiv q = 1.6$, which is approximately the value required for σ^- light to explain our maximum measured value of P_e as discussed in Sec. II. We take the *relative* values
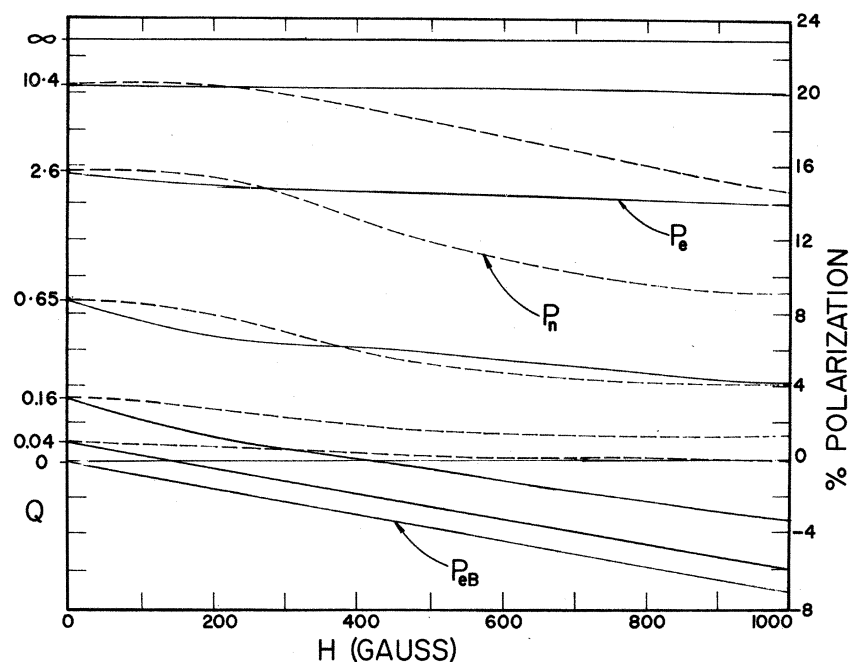
FIG. 9. Computer calculation of P_n and P_e for optical return in case A, $\alpha = 1$, $q = 1.6$, $T = 1.63\,°$K.

$$w_{12} + w_{13} = w_{34} = 0.1, \quad w_{24} = 0.3, \quad w_{14} = w_{23} = 1. \quad (18)$$

We have no good experimental evidence from our experiments for this choice; it is reasonable to assume w_{14} and w_{23} are of order T_{1e}^{-1}, and that the "nuclear" relaxation rates w_{12} and w_{34} are, say, at least an order of magnitude weaker. The relative value $w_{24} > w_{13}$ is consistent with the general results of microwave dynamic polarization experiments[15]; it is furthermore consistent with our experimental result that P_n and P_e always have the same sign. We take $T = 1.63\,°$K to correspond to the experimental value, and solve on an IBM 1620 computer Eqs. (16) for n_1, etc., for various values of the coefficients a^2 and b^2 determined by the field H, and for values of the optical saturation parameter

$$Q \equiv (U_+ + U_-)/w_{14}. \quad (19)$$

The results for the steady-state nuclear polarization P_e and nuclear polarization P_n are plotted vs H in Fig. 9, for various values of Q. At $Q = 0$, $P_e \rightarrow P_{eB} = -g\mu_B H/kT$, which goes to -7.5% at 1 kG. As Q is increased, P_e is decreased in magnitude since σ^- pumping tends to reverse it, and eventually $P_e = P_n = +23\%$ as $Q \rightarrow \infty$. Half this maximum value is obtained when Q is of order unity. As shown in Sec. V, we could experimentally obtain values of Q up to about 30.

Finally, if we further add to the model a strong saturation at rate $W_{24} \gg w_{ij}$, solution of the rate equations shows that for $Q \gg 1$ we again obtain the polarizations of Eqs. (2) and (3) for all fields.

B. Case $\beta = 1$

By omitting w_{ij} and W_{24} terms, the rate equations in this case are easily seen to have the simple solution $n_1 = n_2 = n_3 = n_4 = \frac{1}{4}$, corresponding to zero nuclear and electron polarization. If ground-state relaxation, Eq. (18), is included, the solutions show that P_n remains very small and that P_e is depressed toward zero from its value P_{eB} as Q is increased. The same result holds even if W_{24} is saturated: P_e and P_n remain near zero.

C. Case $\gamma = 1$

This case is what others[40] have called complete reorientation: The return rates are assumed all equal, $R_1 = R_2 = R_3 = R_4$, by a thermalizing mechanism in the pumping cycle. Neglecting W_{24} and w_{ij},

TABLE II. Return rate models for R_i.

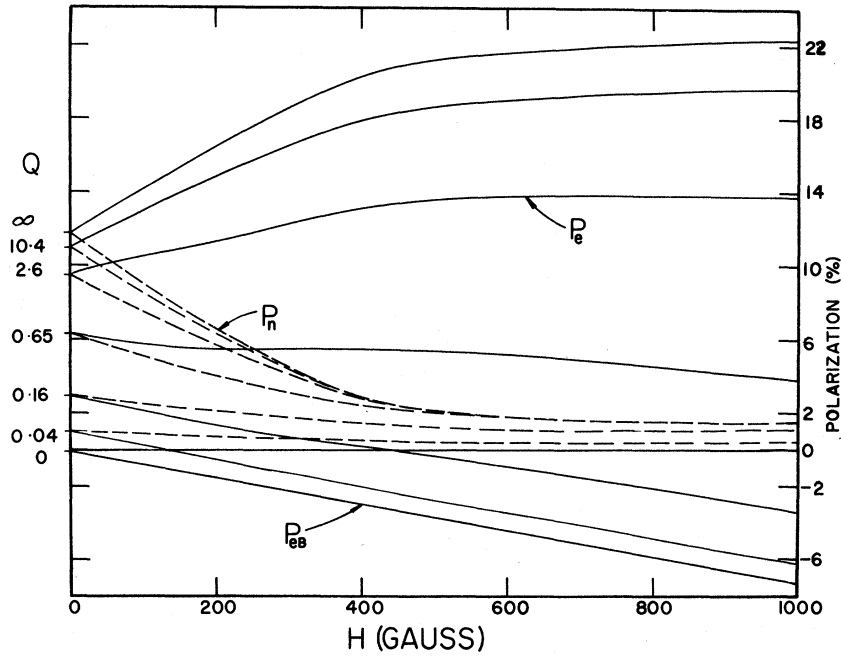| Case	Return relaxation model	Eqs. (17)
A	Complete nuclear-spin memory, randomized electron-spin return	$\alpha = 1$
B	Complete electron-spin memory, randomized nuclear-spin return	$\beta = 1$
C	Randomized nuclear- and electron-spin return, i.e., no spin memory	$\gamma = 1$
D	Complete electron- and nuclear-spin memory	$\delta = 1$

$$\alpha + \beta + \gamma + \delta = 1$$

FIG. 10. Computer calculation of P_n and P_e for optical return in case C, $\gamma=1$, $q=1.6$, $T=1.63$ °K.

the rate equations give the simple solutions

$$P_e = \frac{q-1}{q+1} \frac{a^2b^2(1-6q+q^2)+2q}{a^2b^2(1-q^2)+2q} , \qquad (20a)$$

$$P_n = \frac{(q^2-1)a^2b^2}{(1-q)^2a^2b^2+2q} . \qquad (20b)$$

At high fields, $b^2 \to 0$ and $P_e \to (q-1)/(q+1)$ and $P_n \to 0$. If we now assume the same values of w_{ij}, q, and T as in Fig. 9, we find the steady-state values of P_e and P_n vs H, shown in Fig. 10, for various values of Q. It is clear that $P_n \to 0$ for high fields in marked contrast to case A, Fig. 9.

On the other hand, if we now add the w_{ij}'s and a strong saturation $W_{24} \gg U_+$ for all fields and $Q \gg 1$, one obtains

$$P_e = P_n = (q^2-1)/(q^2+6q+1) . \qquad (21)$$

This shows that saturation of the forbidden transition v_{24} can markedly enhance the nuclear polarization in the case of complete spin reorientation in the optical pumping cycle.

D. Case δ = 1

In this case, "complete spin memory," if $w_{ij}=0$ and $W_{24}=0$, then n_1 and n_3 remain unchanged while n_2 and n_4 become equal. The optical pumping alone is insufficient to determine the populations. At high fields where the rate $w_{14}=w_{23}$ dominates, then $P_n=P_e \approx -\frac{1}{2}\Delta \approx P_{eB}$. This will still hold true if W_{24} is also saturated.

It will be impossible to clearly distinguish the cases experimentally and to determine exactly α, β, γ, and δ. However, we can state at this point

that the data tend to favor case A with a small mixture of case C. This is shown in Fig. 11 for various values of (α, γ) for $q=1.6$, 1.65 °K, $w_{ij}=0$, $W_{24}=0$, calculated by computer including both α and γ terms in Eqs. (17).

V. EXPERIMENTAL RESULTS AND INTERPRETATION

A. Measurements of P_e(Tm^{2+})

An important step in understanding the ^{169}Tm nuclear polarization in CaF$_2$:Tm^{2+} is to first study the electron-spin polarization P_{ep}, from the MCD signal S, defined experimentally by Eq. (13), as a function of H for various pumping intensities of σ^+ and σ^- light, obtained by using neutral density filters (attenuators) in the pump beam. Figure 12 shows some results for crystal No. 1, $\vec{H} \parallel [111]$. The straight line $P_{eB} = -11.2\%$ at 1600 G is the calculated Boltzmann equilibrium value without optical pumping and is used for calibration. The maximum light available corresponds to an optical density OD = 0 attenuator; this gives $P_{ep} = -21$ and $+18\%$, respectively, for σ^+ and σ^- light. There are a number of dips in P_{ep} due to cross relaxation between Tm^{2+} pairs in the range $100 < H < 500$ G, and due to cross relaxations with Ho^{2+} impurities at 1330–1450, 3100–3400, and 6700–7300 G; these have been observed by Sabisky and Anderson.[31,44] These are displayed more fully in Fig. 13 for the same crystal and orientation but in an earlier run.[11] The maximum values of P_{ep} are slightly higher, probably because of better pumping conditions. The maximum value $P_e = -23\%$ for σ^+ light corresponds to $q=0.625$ from Eq. (3), or to $q=1/0.625=1.6$ assuming σ^- light. Actually only $P_{ep}=+20\%$ was
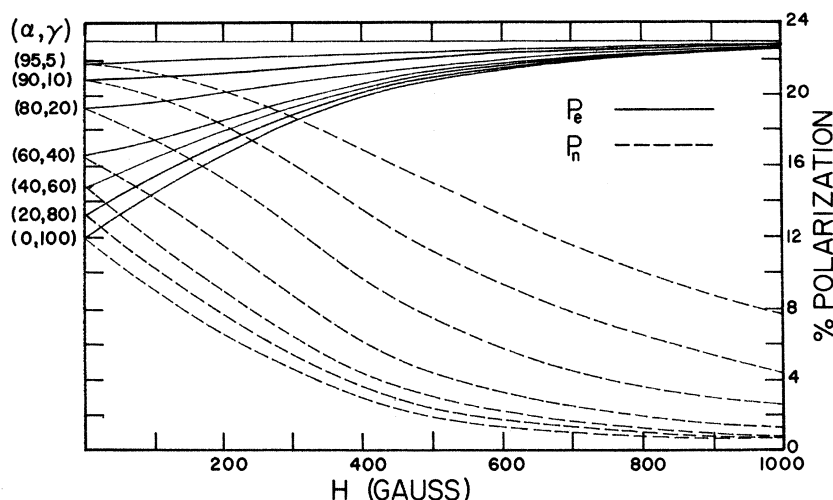
FIG. 11. Computer calculation of P_n and P_e for mixed case A and case C with percentage mixture $(\alpha,\ \gamma)$.

achieved with σ^- light, indicating a lack of full optical saturation.

The cross-relaxation dips in Fig. 13 labeled $a, b, \ldots, f$ are tabulated in Table III and identified by the use of the frequency diagram in Fig. 4 for ν_{ij} of the ground and excited states; the table lists the two transitions, ν_{ij} and ν'_{ij}, which cross at field H_c, along with the actual frequency of ν_{ij}. Also shown in a few cases are the cross-relaxation rate W_{tt} and linewidth σ_{tt}, estimated from the height and width of the dip. Most cross-relaxation dips occur between two $^{169}\text{Tm}^{2+}$ ions in the optical ground state, although some are between a ground-state ion and a metastable state ion. Some dips, e.g., labeled e, are due to three-spin flips. It is likely that at $H \gtrsim 100$ G there is an unresolvable continuum of multispin cross-relaxation dips.

In order to experimentally determine Q, Eq. (19), we measured the buildup rate of P_{ep}, defined by

$T_{bu}^{-1} = T_{1e}^{-1} + T_p^{-1}$, when T_{1e}^{-1} is the decay rate of P_e, i.e., the spin-lattice relaxation rate T_{1e}^{-1} of Fig. 5, and T_p^{-1} is the optical pump rate. It is straightforward to show for a two-level system $(I=0)$ that

$$\frac{T_p^{-1}}{T_{1e}^{-1}} \cong \frac{U_+ + U_-}{4w_{14}} = \frac{Q}{4}. \tag{22}$$

For Fig. 12 at 1.5 kG we measured $T_p^{-1} \approx 6 \text{ sec}^{-1}$, yielding values of Q between 3 and 40 in the range $100 < H < 800$ G, where the nuclear polarization measurements were performed. For Fig. 13, we actually measured a somewhat greater rate, $T_p^{-1} \sim 15 \text{ sec}^{-1}$, although this was not measured as precisely, but is consistent with the larger values of P_{ep}.

B. Measurements of $P_e(^{169}\text{Tm})$

Figure 13, taken at 1.65 °K, also shows our principal experimental result: values of P_{ni} ob-

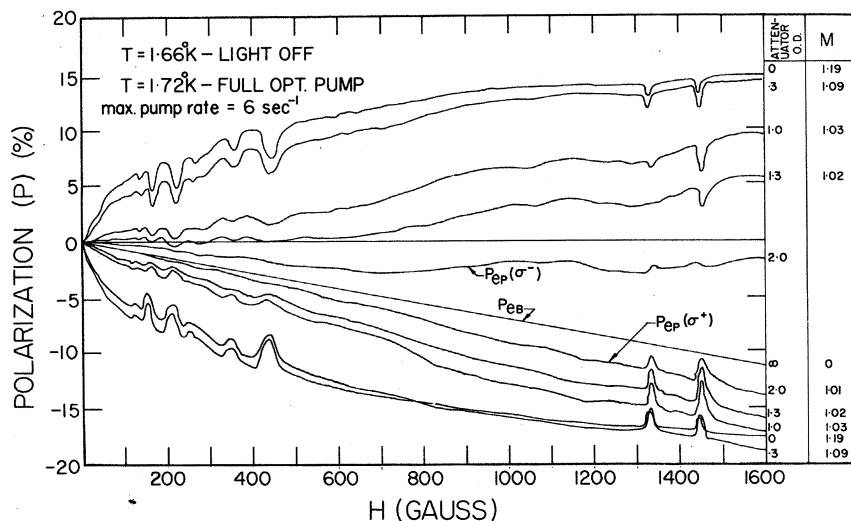

FIG. 12. Direct chart recorder readout of MCD signal S representing electron polarization P_e for crystal No. 1 for pumping with σ^+ and σ^- light through a neutral density filter of OD shown. The curves must be multiplied by the over-all relative gain factor M, shown in the right column, to obtain the true value of P_e.
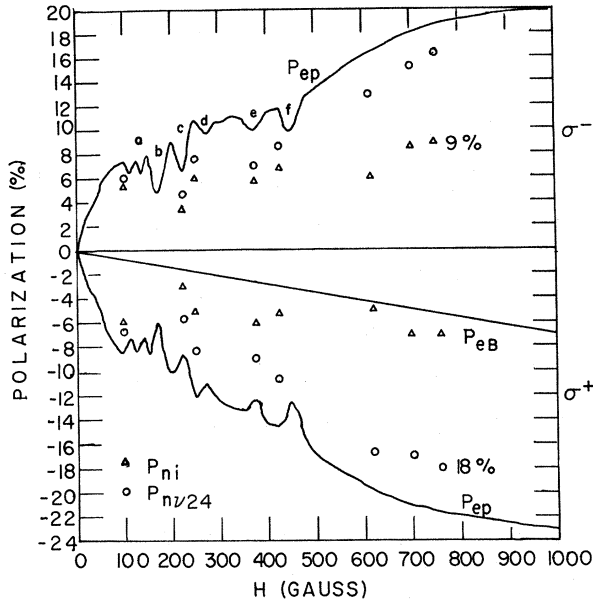
FIG. 13. Smooth lines are measured values of P_e for crystal No. 1 for σ^+ and σ^- light pumping. $\triangle$ are measured values of P_{ni}, the nuclear polarization with optical pumping alone. The open circles are measured values of $P_{n\nu24}$, the nuclear polarization with rf saturation of ν_{24} included. The dips a, b, . . . , f are due to cross relaxation between pairs or triplets of Tm^{2+} ions.

tained with only optical pumping, and values of $P_{n\nu24}$ obtained by additional rf saturation of ν_{24}. The maximum value, at 750 G, is $P_{ni} = 9\%$ for σ^- light; for σ^+ light we measure $P_{ni} = -7\%$. With W_{24} added, we find $P_{n\nu24} = 16\%$ for σ^- light, and $P_{n\nu24} = -18\%$ for σ^+ light. The latter value is enhanced by a factor 910 over the thermal-equilibrium value. Closer examination of Fig. 13 shows that P_{ni} and $P_{n\nu24}$ are reduced, along with P_{ep}, near the cross-relaxation dips, as expected. With some scatter, one can say that roughly P_{ni} is approximately $\frac{1}{2}P_{ep}$ for σ^-

light, and approximately $\frac{1}{3}P_{ep}$ for σ^+ light. The fact that P_{ni} and P_e always have the same sign is consistent with the assumption $w_{24} > w_{13}$, as indicated in the elementary discussion in Sec. I. The asymmetry in $|P_{ni}|$ is also consistent with this assumption and arises from the fact that for σ^- light P_{ni} predicted by Eq. (4) is larger than P_e due to the fact that Δ is not negligible at the low temperatures used. That the observed values of P_{ni} are less than P_e indicates that the assumption $w_{24} \gg w_{13}$ is not valid, but still $w_{24} > w_{13}$ is valid.

It is rather hopeless to attempt a quantitative explanation of the results for P_n since we do not actually know the w_{ij} values, which very likely depend on the H field, nor do we know α, β, γ, and δ, also possibly field dependent. But a few statements can be made: The only optical relaxation model in which large values of P_n are obtained in high fields, e. g., 750 G, without rf saturation is case A: nuclear-spin memory, randomized electron-spin decay. Furthermore, if we saturate ν_{24}, then only cases A and C will yield sizable values of P_n; but case C is limited to $P_n \approx -12\%$ from Eq. (21), whereas we observe -18%, which is closer to the expected value for pure case A, -21.5%, the maximum observed value of P_{ep} at 750 G. This suggests that a mixture of the two cases, say $(\alpha, \gamma) \approx (0.9, 0.1)$, may be necessary to explain the values of P_{ni} at 750 G (see Fig. 11). At the low fields, $H < 200$ G, the rapid fall-off of P_{ep} and P_{ni} must be due to lack of optical saturation, and to increased cross relaxation, as strongly suggested by T_{1e}^{-1} from Fig. 5: T_{1e}^{-1} increases by a factor 10 as H goes from 1000 to 100 G. Also, the degree of nuclear-spin memory probably falls off at low fields. We further note that the measured values of Q in Eq. (22) were roughly consistent with the saturation behavior of the polarization.

To summarize, we have demonstrated that sizable nuclear polarizations of up to 18% can be

TABLE III. Tm^{2+} cross-relaxation data.

H_c (G)	Label (Fig. 13)	ν_{ij} (MHz)	ν_{ij} (label)	ν'_{ij} (label)	Observed in Tm^{2+} expt (crystal No. 1)	Observed in ^{19}F expt (crystal No.2)	W_{tt} (sec^{-1})	σ_{tt} (MHz)
131	a	1270	ν_{24}	$2\nu_{13}$	yes	no		
135	a	860	ν_{34}	$2\nu_{23}$	yes	no		
169	b	830	ν_{13}	ν_{34}	yes	yes	60	21 ± 4
225	c	780	ν_{23}	ν_{34}	yes	yes	60	21 ± 4
264	d	950	ν_{23}	ν^*_{12}	yes	yes		
265	d	1280	ν_{13}	ν^*_{13}	yes	yes		
283		360	ν_{12}	ν^*_{23}	yes	yes		
300		220	ν_{14}	$2\nu_{23}$	yes	no		
304		1460	ν_{13}	$2\nu_{34}$	yes	yes		
346		710	ν_{34}	ν^*_{24}	yes	yes		
371	e	1420	ν_{23}	$2\nu_{34}$	yes	yes	20 ± 10	39 ± 5
452	f	1780	ν_{23}	ν^*_{14}	yes	yes		

achieved; these can be compared to the 21.5% maximum value of P_e for our conditions for $CaF_2: Tm^{2+}$. This was only achieved by optical pumping plus rf saturation of ν_{24}; with only optical pumping the nuclear polarization is reduced by a factor 2, indicating that the assumption of complete nuclear-spin memory in case A made in deriving Eq. (4) is not really valid, and that perhaps 10% of the optical return is via case C, which has no spin memory. We can conclude that a high degree of nuclear-spin memory exists in the optical pumping cycle, of order 90% at 750 G.

VI. POLARIZATION OF ^{19}F BY OPTICAL PUMPING

A. Theory

The idea of polarization of the abundant ^{19}F nuclei by a three-spin cross relaxation with a pair of optically pumped ^{169}Tm^{2+} ions, introduced in qualitative way in Sec. I and Fig. 2, can be made quantitative by adopting a Gibbs approach of viewing this process in terms of the product states of a three-spin system,[18] or by the usual cross-relaxation rate-equation approach,[45,46] which we use here, focusing our attention on a specific but representative crossing: $\nu_{23} = \nu_{34}$ at 224 G, dip c in Fig. 3. The previous work which is most like ours is that of Atsarkin et al.[47] on microwave resonance and cross relaxation in ruby. It should be stated im-

mediately that Fig. 3 is highly idealized in that it assumes that the intrinsic width $\delta\nu_1$ of the hfs energy levels is small compared to the ^{19}F frequency ν_3; in fact just the reverse is true: $\delta\nu_1 \approx \delta\nu_2 \gg \nu_3$. This means that the ^{19}F polarization will be only a differential effect, reduced by the factor $(\nu_3/\delta\nu_1)$. Also the separation ΔH between maxima and minima of $P_n(^{19}$F$)$ will not occur at $\Delta H \sim (g_n/g)H$, but will be pushed apart to a value $\Delta H \sim h\delta\nu_1/g\beta$. These intuitive expectations follow by analogy to dynamic microwave polarization experiments involving saturation of forbidden lines which are not resolved,[41] and are also consistent with the following cross-relaxation theory.

The rate equations will involve two ^{169}Tm^{2+} ions (a primed and an unprimed set) and one ^{19}F ion. Let all the single-ion terms in Eqs. (16) be represented by terms of the form $\dot{n}_j = \sum_i (n_i V_i^j - n_j V_j^i)$. Let $\Delta = h\nu_{23} - h\nu'_{34}$ be the energy mismatch of the crossing, and $\delta = g_n\mu_B H$ be ^{19}F nuclear Zeeman splitting. The rate equations, including two-ion Tm-Tm cross-relaxation rate W_{tt}, and three-ion Tm-Tm-F cross-relaxation rate W_{ttf}, can be written assuming Gaussian cross-relaxation linewidths σ_{tt} and σ_{ttf}, respectively. We obtain

$$\frac{dn_1}{dt} = \sum_{i \neq 1} (-n_1 V_1^i + n_i V_i^1) , \tag{23a}$$

$$\frac{dn_2}{dt} = \sum_{i \neq 2} (-n_2 V_2^i + n_i V_i^2) - W_{tt}(n_2 n_4' - n_3 n_3') e^{-\Delta^2/2\sigma_{tt}^2} - W_{ttf}(n_2 n_4' n_- - n_3 n_3' n_+) e^{-(\Delta+\delta)^2/2\sigma_{ttf}^2}$$

$$- W_{ttf}(n_2 n_4' n_+ - n_3 n_3' n_-) e^{-(\Delta-\delta)^2/2\sigma_{ttf}^2} , \tag{23b}$$

$$\frac{dn_3}{dt} = \sum_{i \neq 3} (-n_3 V_3^i + n_i V_i^3) + W_{tt}(n_2 n_4' - n_3 n_3') e^{-\Delta^2/2\sigma_{tt}^2} + W_{tt}(n_2' n_4 - n_3' n_3) e^{-\Delta^2/2\sigma_{tt}^2}$$

$$+ W_{ttf}(n_2 n_4' n_- - n_3 n_3' n_+) e^{-(\Delta+\delta)^2/2\sigma_{ttf}^2} + W_{ttf}(n_2' n_4 n_- - n_3' n_3 n_+) e^{-(\Delta+\delta)^2/2\sigma_{ttf}^2}$$

$$+ W_{ttf}(n_2 n_4' n_+ - n_3 n_3' n_-) e^{-(\Delta-\delta)^2/2\sigma_{ttf}^2} + W_{ttf}(n_2' n_4 n_+ - n_3' n_3 n_-) e^{-(\Delta-\delta)^2/2\sigma_{ttf}^2} , \tag{23c}$$

$$\frac{dn_4}{dt} = \sum_{i \neq 4} (-n_4 V_4^i + n_i V_i^4) - W_{tt}(n_2' n_4 - n_3 n_3') e^{-\Delta^2/2\sigma_{tt}^2} - W_{ttf}(n_2' n_4 n_- - n_3 n_3' n_+) e^{-(\Delta+\delta)^2/2\sigma_{ttf}^2}$$

$$- W_{ttf}(n_2' n_4 n_+ - n_3 n_3' n_-) e^{-(\Delta-\delta)^2/2\sigma_{ttf}^2} . \tag{23d}$$

There is another set of four equations which are identical in form to Eq. (23) but with the primed and unprimed n_i interchanged.

Then there are the fluorine rate equations, which have terms for ground-state relaxation at rate w_F and cross relaxation from the Tm^{2+} system:

$$\frac{dn_-}{dt} = -n_- w_F e^{-\delta/kT} + n_+ w_F - W_{ttf}(n_2 n_4' n_- - n_3 n_3' n_+) e^{-(\Delta+\delta)^2/2\sigma_{ttf}^2} - W_{ttf}(n_2' n_4 n_- - n_3' n_3 n_+) e^{-(\Delta+\delta)^2/2\sigma_{ttf}^2}$$

$$+ W_{ttf}(n_2 n_4' n_+ - n_3 n_3' n_-) e^{-(\Delta-\delta)^2/2\sigma_{ttf}^2} + W_{ttf}(n_2' n_4 n_+ - n_3' n_3 n_-) e^{-(\Delta-\delta)^2/2\sigma_{ttf}^2} , \tag{24a}$$

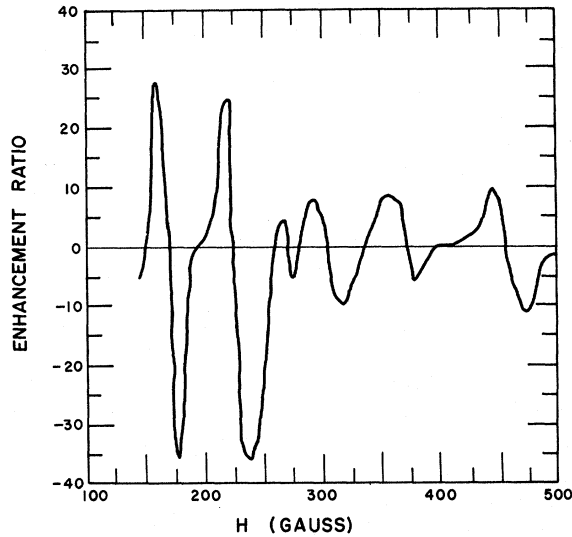$$-\frac{dn_+}{dt} = \frac{dn_-}{dt} . \tag{24b}$$

FIG. 14. Measured enhancement of ^{19}F nuclear polari-
zation at 1.9 °K through cross relaxation with σ^+ optically
pumped ^{169}Tm^{2+} ions.

In calculating the fluorine polarizations, these
equations form the basis for a simple computer
method of solution. First, the primed populations
n_i' are set equal to the unprimed ones. We define
the ^{19}F nuclear polarization P_F, and solve Eq. (24)
to obtain in the steady state

$$E_+ \equiv \exp\left[-\frac{(h\nu_{23} - h\nu_{34} + \delta)^2}{2\sigma_{ttf}^2}\right] , \tag{25a}$$

$$E_- \equiv \exp\left[-\frac{(h\nu_{23} - h\nu_{34} - \delta)^2}{2\sigma_{ttf}^2}\right] , \tag{25b}$$

$$P_F \equiv \frac{n_- - n_+}{n_- + n_+}$$

$$= \frac{w_F(1 - e^{-\delta/kT}) + W_{ttf}(n_2 n_4 - n_3^2)(E_+ - E_-)}{2W_{rf} + w_F(1 + e^{-\delta/kT}) + W_{ttf}(n_2 n_4 + n_3^2)(E_+ + E_-)} . \tag{25c}$$

To determine n_2, n_3, and n_4 in Eq. (25), we use the
thulium parameters V_i^j as determined from the
theory of Sec. IV and the general experimental re-
sults. Then W_{tt} and σ_{tt} are determined from the
cross-relaxation dips in P_{ep}. The relaxation rate
can be found by experiment, and σ_{ttf} can be set
equal to σ_{tt} because $\delta \ll \sigma_{tt}$ so that the one remain-
ing parameter (determined later by computer fit)
is W_{ttf}.

B. Experimental Results and Interpretation

The primary experimental results are shown in
Fig. 14, obtained on crystal No. 2 at $T \approx 1.9$ °K
while pumping with σ^+ light in the 5400–6000-Å
band. The direct NMR resonance of ^{19}F was mea-
sured at thermal equilibrium at some field H with-
out optical pumping; then the light was turned on
and the NMR signal measured again. The observed
enhancement ratio vs H is plotted, and shows the
general features expected: At 169 G (see Table III)
there is a ν_{13}, ν_{34}' crossing, dip b Fig. 13, with the
enhancement going positive and then negative, in
agreement with Fig. 2. At 225 G there is the ν_{23},
ν_{34}' crossing studied in detail, dip c, etc., for a
number of other crossings, some weaker ones in-
volving a Tm ion in the optically excited state and
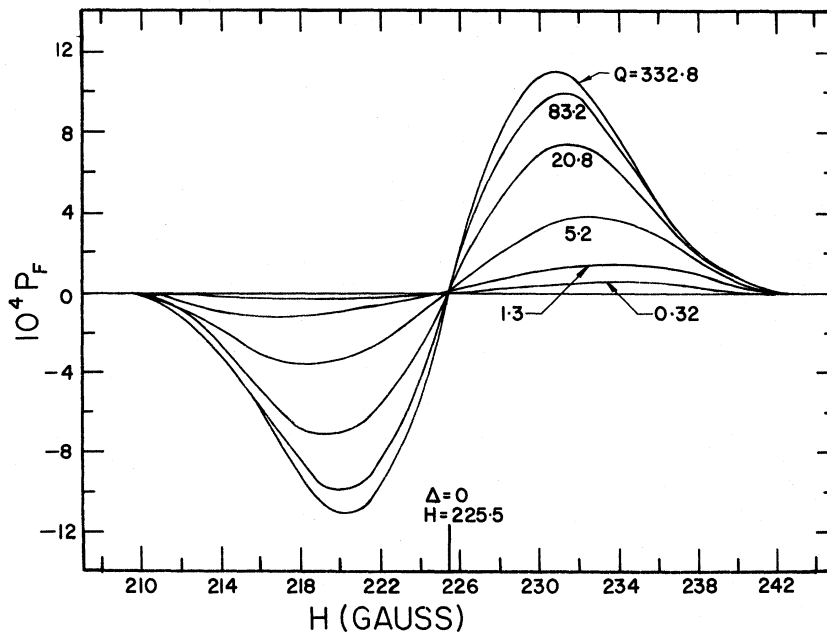some even involving three Tm ions, i.e., a four-

FIG. 15. Computer calculation
of rate-equation model to explain
Fig. 14.

spin cross relaxation. Using σ^- light reversed the sign of the enhancement, as expected. With optical pumping alone enhancements up to 40× were observed. This could be increased up to a factor 2 by also saturating some of the rf transitions, but this was not studied in detail.

To compare the results at the 225 G crossing with theory we evaluate Eq. (25c) as discussed above using the parameters $\sigma_{tt} \approx \sigma_{ttf} = 24$ MHz, $W_{tt} \approx 60$ sec^{-1}, $w_{14} = 4$ sec^{-1}, $w_F = 0.07$ sec^{-1}, $U_+ = 6$ sec^{-1}, all measured; and the following assumed values: $w_{13} = w_{12} = w_{34} = 0.8$ sec^{-1}, $w_{23} = w_{14} = 4$ sec^{-1}, $w_{24} = 1.2$ sec^{-1}, $\alpha = 0.7$, $\gamma = 0.3$, and $q = 1.6$ for σ^- light. W_{ttf} was estimated to be ~ 0.1 sec^{-1} from the measured buildup rate of P_F. The resulting value for P_F vs H near the crossing is plotted in Fig. 15 for various values of the optical saturation parameter Q. The thermal-equilibrium polarization is $P_{F_0} = 0.13 \times 10^{-4}$. Within the limitations of this many-parameter theory, the agreement with the data is satisfactory; the magnitude of P_F and the spacing between peaks is reasonably explained. The theoretical value $P_F = 4 \times 10^{-4}$, for $Q \approx 5$ shown in Fig. 15, corresponds to an enhancement of 31 in Fig. 14. Also the spacing $\Delta H = 14$ G between maxima and minimum of P_F in Fig. 15 corresponds approximately with the measured values of 19 G.

Although the maximum ^{19}F polarizations that were achieved, $P_n \approx 0.1\%$, are quite small and entirely insignificant compared to the values $P_n \approx 50\%$ obtained by microwave dynamic polarization, [49] nevertheless it is seen that, in principle, larger polarizations could be obtained in high fields where the linewidth $\sigma_{ttf} < \nu_{\text{nuc}}$, so that the full optically pumped polarization P_e could be transferred to the nuclei. Such crossings do not exist in CaF$_2$: ^{169}Tm^{2+}, but might in other crystals.

APPENDIX

The problem to be treated in this Appendix will be the calculation of spin-lattice relaxation rates $w_{ij} = T_{1d}^{-1}|_{ij}$, Fig. 1, for the four ground-state hfs levels of CaF$_2$: ^{169}Tm in arbitrary field $\vec{H}$ due to the direct process. This can be done by extending the calculation of Sabisky and Anderson[31] to include the hfs interaction, using the procedures of Baker

and Ford, [50] and Larson and Jeffries. [51] For the Kramers doublet Tm^{2+} the direct process occurs only through admixtures of the $G_{3/2}$ state at 555.8 cm^{-1} into the $E_{5/2}$ ground state, by the Zeeman and hfs Hamiltonian

$$\mathcal{3C}_1 = g_L \beta \vec{H} \cdot \vec{J} + a \vec{I} \cdot \vec{J} , \tag{A1}$$

where $g_L = \frac{8}{7}$ in the Landé g factor; a is related to the hfs constant A in the effective-spin Hamiltonian, Eq. (1), by $a = A g_L / g$; and $J = \frac{7}{2}$ for the $^2F_{7/2}$ multiplet. We will do the calculation for the orientation $H \parallel [001]$ for which $\vec{H} \cdot \vec{J} \rightarrow H J_z$. The first term in Eq. (A1) splits the $E_{5/2}$ ground state into the Zeeman doublet $|a\rangle$ and $|b\rangle$, and the $G_{3/2}$ state into the quartet $|p_{11}\rangle$, $|p_{12}\rangle$, $|p_{13}\rangle$, and $|p_{14}\rangle$, all given explicitly by Huang's Eq. (29), [30] in terms of $|J = \frac{7}{2}$, $J_z\rangle$ basis states. To take hfs into account we replace $|a\rangle$ and $|b\rangle$ by four ground-state functions ψ_{0i} of the form of Eqs. (5), diagonal in $\mathcal{3C}_1$, with $|M_S = -\frac{1}{2}\rangle$ and $|M_S = +\frac{1}{2}\rangle$ replaced by $|a\rangle$ and $|b\rangle$, respectively. Similarly we replace the $|p_{11}\rangle$, etc., by eight functions ψ_{ek} for the $G_{5/2}$ excited state. The direct process is then given by the expression[51,31]

$$w_{ij} = \frac{1}{T_{1d}}\bigg|_{ij} = \frac{2}{2\pi\rho v_t^5 \hbar} \left(\frac{h\nu_{ij}}{\hbar}\right)^3 \bigg| \sum_k \frac{2}{\Delta_{ik}}$$

$$\times \left[\langle \psi_{0i} | \mathcal{3C}_1 | \psi_{ek} \rangle \langle \psi_{ek} | \sum_{n,m} V_n^m | \psi_{0j} \rangle + \langle \psi_{0i} | \sum_{n,m} V_n^m | \psi_{ek} \rangle \right.$$

$$\left. \times \langle \psi_{ek} | \mathcal{3C}_1 | \psi_{0i} \rangle \right] \bigg|^2 \coth(h\nu_{ij}/2kT) \text{ sec}^{-1} , \tag{A2}$$

where ν_{ij} is the ground-state frequency difference, Fig. 4; $\Delta_{ik} \approx 555$ cm^{-1} is the crystal-field splitting; ρ is the crystal density; v_t is the transverse sound velocity; and $\sum V_n^m$ is the orbit-lattice interaction given by $\sum A_n^m O_n^m$, where O_n^m are Orbach's operators, [34] and A_n^m are magnitudes, best determined from the measurements of Sabisky and Anderson. [31] For the XY_8 complex of CaF$_2$ the normal modes transform like T_{2g}, leading to $V_{n=2,4,6}^{m=\pm1,2}$ terms; and like E_g, leading to $V_{n=2,4,6}^{m=0,2}$ terms. The over-all result is that only T_{2g} vibrations contribute to w_{12}, w_{14}, w_{23}, and w_{34}. These are evaluated[19] using $^{T_{2g}}A_2^1 \langle \psi_e | O_2^1 | \psi_0 \rangle = 308$ cm^{-1} and $^{T_{2g}}A_2^2 \langle \psi_e | O_2^2 | \psi_0 \rangle = 200$ cm^{-1} and plotted in Fig. 6, assuming $\coth(h\nu_{ij}/2kT) \approx 2kT/h\nu_{ij}$ and taking $T = 1°$K. Only E_g vibrations contribute to w_{24}, which was evaluated and plotted using $^{E_g}A_2^0 \langle \psi_0 | O_2^2 | \psi_0 \rangle = 250$ cm^{-1} and $^{E_g}A_2^2 \langle \psi_e | O_2^2 | \psi_0 \rangle = 450$ cm^{-1}. Both T_{2g} and E_g vibrations contribute to w_{13}, which is plotted in Fig. 6 using only E_g contributions; the T_{2g} contributions will approximately double this rate. As expected, w_{23} and w_{14} at high fields become the rate $T_{1e}^{-1} \propto H^4 T$, as measured and plotted in Fig. 5. The ^{169}Tm nuclear relaxation rates w_{12} and w_{34} remain very weak, and w_{13} and w_{24} are intermediate.

*Work supported in part by the U. S. Atomic Energy Commission, Report No. UCB-34P20-142.

†Present address: Freie Universität Berlin, IV. Physikalisches Institut, 1 Berlin 33, Boltzmanstr. 20, Germany.

[1]Static methods, e. g., D. A. Shirley, Ann. Rev. Nucl. Sci. 16, 89 (1966).

[2]Dynamic methods, e. g., *Proceedings of the International Conference on Polarized Targets and Ion Sources, Saclay, 1966* (Centre d'Etudes Nucléarires de Saclay, Saclay, France, 1967).

[3]A. Kastler, J. Phys. Radium 11, 255 (1950).

[4]C. Cohen-Tannoudji and A. Kastler, *Progress in Optics*, edited by E. Wolf (North-Holland, Amsterdam, 1966).

[5]F. D. Colegrave, L. D. Shearer, and G. K. Walters, Phys. Rev. 132, 2561 (1963).

[6]G. W. Series and M. S. Taylor, J. Phys. Radium 19, 901 (1958).

[7]N. V. Karlov, J. Margerie, and V. Merle D'Aubigne, J. Phys. (Paris) 24, 717 (1963).

[8]J. Margerie, *Electronic Magnetic Resonance and Solid Dielectrics* (North-Holland, Amsterdam, 1964), p. 69.

[9]C. D. Jeffries, in *Hyperfine Structure and Nuclear Radiations*, edited by E. Matthias and D. Shirley (North-Holland, Amsterdam, 1968), p. 775; C. D. Jeffries, Phys. Rev. Letters 19, 1221 (1967).

[10]C. H. Anderson, H. A. Weakliem, and E. S. Sabisky, Phys. Rev. 143, 223 (1966).

[11]L. F. Mollenauer, W. B. Grant, and C. D. Jeffries, Phys. Rev. Letters 20, 488 (1968).

[12]G. Lampel, Phys. Rev. Letters 20, 491 (1968).

[13]G. Maier, U. Haeberlen, H. C. Wolf, and K. H. Hausser, Phys. Letters 25A, 384 (1967).

[14]R. G. Bessent and W. Hayes, Proc. Roy. Soc. (London) 285, 430 (1965).

[15]C. D. Jeffries, Phys. Rev. 106, 164 (1957); 117, 1056 (1960).

[16]A. Abragam, Phys. Rev. 98, 1729 (1955).

[17]A. Overhauser, Phys. Rev. 92, 411 (1953).

[18]W. B. Grant, R. L. Ballard, and L. F. Mollenauer, University of California, Berkeley, Technical Report No. UCB-34P20-T2, 1968 (unpublished).

[19]W. B. Grant, thesis (University of California, Berkeley, Technical Report No. UCB-34P20-T6, 1971) (unpublished).

[20]P. W. Bridgman, Proc. Am. Acad. Arts Sciences 60, 303 (1925); D. C. Stockbarger, Rev. Sci. Instr. 7, 133 (1936).

[21]W. Hayes and J. W. Twidell, J. Chem. Phys. 35, 1521 (1961).

[22]D. W. McClure and Z. J. Kiss, J. Chem. Phys. 39, 3251 (1963).

[23]See J. H. Schulman and W. D. Compton, *Color Centers in Solids* (Pergamon, New York, 1962), p. 38.

[24]Z. J. Kiss and P. N. Yocom, J. Chem. Phys. 41, 1511 (1964).

[25]W. Low, J. Phys. Soc. Japan Suppl. 17, 440

(1962).

[26]Z. J. Kiss, Phys. Rev. 127, 718 (1962).

[27]E. S. Sabisky and C. H. Anderson, Phys. Rev. 148, 194 (1966).

[28]B. Bleaney, Proc. Roy. Soc. (London) A277, 289 (1964).

[29]E. S. Sabisky and C. H. Anderson, J. Quant. Electron. QE-3, 287 (1967).

[30]Chao-Yuan Huang, Phys. Rev. 139, A241 (1965).

[31]E. S. Sabisky and C. H. Anderson, Phys. Rev. B 1, 2028 (1970).

[32]D. S. McClure, S. R. Polo, and H. A. Weakleim, *Electronic Spectra of Transition Metal Ions in Crystals* (U. S. Department of Commerce, Office of Technical Services, Washington, 1961).

[33]H. A. Weakliem, C. H. Anderson, and E. S. Sabisky, Phys. Rev. B 2, 4354 (1970).

[34]R. Orbach, Proc. Roy. Soc. (London) A264, 456 (1961).

[35]P. L. Scott and C. D. Jeffries, Phys. Rev. 127, 32 (1962).

[36]L. F. Mollenauer, C. D. Grandt, W. B. Grant, and H. Panepucci, Rev. Sci. Instr. 39, 1958 (1968).

[37]L. F. Mollenauer, D. Downie, H. Engstrom, and W. B. Grant, Appl. Opt. 8, 661 (1969).

[38]J. O. Kemp (private communication). See, also, S. N. Jasperson and S. E. Schnatterly, Rev. Sci. Instr. 40, 76 (1969).

[38a]P. D. Parry, T. R. Carver, S. O. Sari, and S. E. Schnatterly, Phys. Rev. Letters 22, 326 (1968).

[39]J. Mort, F. Lüty, and F. C. Brown, Phys. Rev. 137, A566 (1963).

[40]W. Franzen and A. G. Emslie, Phys. Rev. 108, 1453 (1957).

[41]G. F. Imbusch, S. R. Chinn, and S. Geschwind, Phys. Rev. 161, 295 (1967).

[42]L. F. Mollenauer, S. Pan, and S. Yngvesson, Phys. Rev. Letters 23, 683 (1969).

[43]C. H. Anderson and E. S. Sabisky, Phys. Rev. 178, 547 (1969).

[44]E. S. Sabisky and C. H. Anderson, *Physical Acoustics* (Academic, New York, to be published).

[45]N. Bloembergen, S. Shapiro, P. S. Pershan, and J. O. Artman, Phys. Rev. 114, 445 (1959).

[46]P. S. Pershan, Phys. Rev. 117, 109 (1960).

[47]V. A. Atsarkin, A. E. Mefed, and M. I. Rodak, Zh. Eksperim. i Teor. Fiz. Pis'ma v Redaktsiyu 6, 942 (1967) [Sov. Phys. JETP Letters 6, 359 (1967)]; Phys. Letters 17A, 57 (1968).

[48]See, e. g., C. D. Jeffries, *Dynamic Nuclear Orientation* (Wiley, New York, 1963), p. 134.

[49]M. Chapellier, M. Goldman, Vu Hoang Chau, and A. Abragam, Compt. Rend. (to be published).

[50]J. M. Baker and N. C. Ford, Phys. Rev. 136, A1692 (1964).

[51]G. H. Larson and C. D. Jeffries, Phys. Rev. 145, 311 (1966).